

Leveraging Temporal Contextualization for Video Action Recognition

Minji Kim^{1†} Dongyoon Han³ Taekyung Kim^{3*} Bohyung Han^{1,2*}

¹ECE & ²IPAI, Seoul National University ³NAVER AI Lab

Abstract. Pretrained vision-language models have shown effectiveness in video understanding. However, recent studies have not sufficiently leveraged essential temporal information from videos, simply averaging frame-wise representations or referencing consecutive frames. We introduce Temporally Contextualized CLIP (TC-CLIP), a pioneering framework for video understanding that effectively and efficiently leverages comprehensive video information. We propose Temporal Contextualization (TC), a novel layer-wise temporal information infusion mechanism for video that extracts core information from each frame, interconnects relevant information across the video to summarize into context tokens, and ultimately leverages the context tokens during the feature encoding process. Furthermore, our Video-conditional Prompting (VP) module manufactures context tokens to generate informative prompts in text modality. We conduct extensive experiments in zero-shot, few-shot, base-to-novel, and fully-supervised action recognition to validate the superiority of our TC-CLIP. Ablation studies for TC and VP guarantee our design choices. Code is available at <https://github.com/naver-ai/tc-clip>.

1 Introduction

Pretrained large-scale Vision-Language Models (VLMs) have shown remarkable generalization capability in video understanding and have emerged as promising tools even for zero-shot or open-vocabulary recognition tasks [10, 24, 36]. However, pretraining task-specific models using video-text pairs pose significant challenges, primarily due to substantial computational costs as well as excessive expense for annotated video-text data [31, 34]. Consequently, recent studies in video understanding [5, 9, 13, 22, 26, 30, 32, 33] have shifted their focus towards employing image-based VLMs such as CLIP [24] via fine-tuning—aligning video representations with text embeddings derived from category names.

Despite the successful generalization of CLIP in video recognition, existing approaches fail to fully exploit temporal information in the video feature learning process. Specifically, the token interactions remain restrictive since they either rely on simple averaging of frame-wise representations [26], or attempt to gather information in the temporal axis only through class tokens [22, 32] as illustrated

[†]Work done during an internship at NAVER AI Lab.

*Corresponding authors.

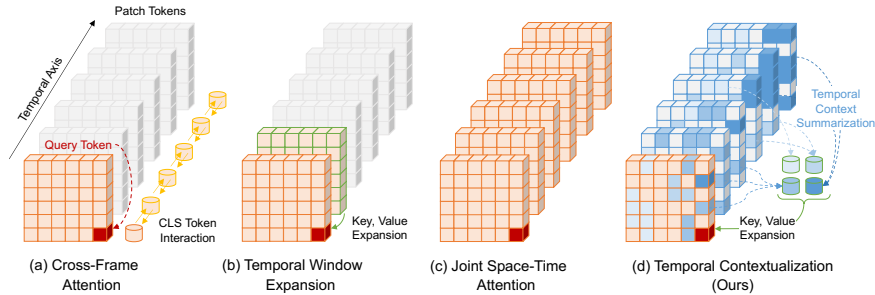


Fig. 1: Temporal information learning methods. Prior works considered temporal cues during the encoding process via (a) cross-frame attention [22,32] with [CLS] token interactions or (b) temporal window expansion [33] by adding adjacent frame tokens to key-value pairs. However, the former lacks patch-level interactions, while the latter limits the range of temporal locality. (c) joint space-time attention allows full interactions across all tokens, but it is costly and incurs suboptimal performance (see Fig. 3). (d) Unlike prior approaches, our method aggregates pivotal tokens from a broader range yet efficiently for enhanced temporal integration into key-value pairs.

in Fig. 1(a). Although VCLIP [33] incorporates patch-level details by bringing keys and values from neighborhood frames in its self-attention operation, as in Fig. 1(b), its temporal scope is still limited to a local window. Such naïve computation for video representations makes models biased towards static information in their representation learning (e.g., objects and backgrounds) and hampers learning temporal information (e.g., motion and temporal variations). To ensure the global interactions of patch tokens in a spatio-temporal domain, one possible option is to consider every patch token from all frames as a reference during the encoding process as illustrated in Fig. 1(c).

Unfortunately, such a straightforward extension for temporally global interactions in VLMs pretrained with short image-text pairs witnesses extrapolation challenges [4, 23] due to the huge number of tokens in each video. We have observed that a naïve extension of sequence length along the temporal axis degrades its discriminability substantially, as shown in Fig. 2. The joint space-time attention model distributes its attention broadly across the patches but fails to concentrate on informative tokens to recognize actions, incurring suboptimal performance compared to the frame-wise attention baseline. Moreover, this approach suffers from heavy computational overhead due to numerous redundant and similar tokens often corresponding to background regions.

This paper presents **Temporally Contextualized CLIP (TC-CLIP)**, a novel paradigm for extending CLIP to the video domain by encoding holistic video information through advanced temporal analysis. Specifically, our Temporal Contextualization (TC) pipeline summarizes global-range action cues into a small set of tokens for reference during the encoding process. Based on the simple idea by utilizing [CLS] query for self-attention, we could extract informative tokens from each frame and group them contextually. These context tokens act as additional key-value pairs for attention operations in the subsequent layer, presumably serving as a temporal bridge that conveys the video-level context

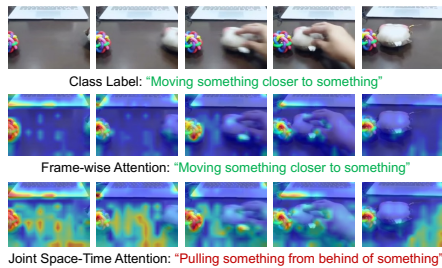


Fig. 2: Pitfall of joint space-time attention. Extending CLIP’s temporal sequence length degrades attention quality, presumably because it was not trained on such long sequences.

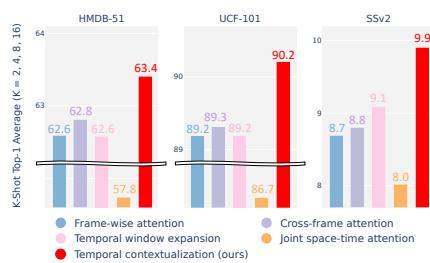


Fig. 3: Quantitative analysis on temporal modelings. We compare the action recognition performance in the few-shot settings on diverse datasets. All existing methods fall behind our method.

throughout the encoding process. Our preliminary study, shown in Fig. 3, implies that existing methods shown in Fig. 1 offer minimal improvement over the frame-wise attention, highlighting the need for enhanced token interactions.

Furthermore, we propose the Video-conditional Prompting (VP) module for the generation of instance-level textual prompts based on produced context tokens. The VP module is composed of cross-attention operations that adopt learnable text prompts as queries and visual temporal tokens as keys and values for injecting video instance representations into video-conditional textual prompts. This strategy alleviates the lack of textual semantics in video action recognition datasets, where category names are the only descriptions of actions (e.g., skateboarding, skydiving, ski jumping), without detailed narratives about acting subjects, observed objects and environment, etc.

To verify the effectiveness and robustness of TC-CLIP, we provide extensive evaluations across five different benchmarks—Kinetics-400 [16] & 600 [2], HMDB-51 [18], UCF-101 [28], and Something-Something v2 [8]. Quantitative comparisons in zero-shot, few-shot, base-to-novel, and fully-supervised experiments show that the proposed approach outperforms the state-of-the-art methods with significant margins of 0.9%p, 1.9%p, 2.0%p, and 0.5%p, respectively, on average. In particular, our zero-shot recognition accuracy on HMDB-51, UCF-101, and Kinetics-600 achieves 54.2%, 82.9%, and 75.8%, respectively, and is further improved by utilizing Large Language Model (LLM)-based text augmentations, recording 56.0%, 85.4%, and 78.1%. We also provide an in-depth analysis of our design choices and the impact of each component in our model.

2 Related Work

CLIP for video action recognition. Recent video understanding studies [5, 9, 13, 20, 22, 26, 30, 32, 33] focus on adapting language-image pre-trained models [10, 24, 36]. As a pioneering work, ActionCLIP [30] introduces CLIP [24] into video recognition by adding temporal attention layers after the backbone in a late-fusion fashion. To consider global-range temporal cues during feature encod-

ing, X-CLIP [22] and Vita-CLIP [32] perform cross-frame attention, promoting [CLS] token interaction before spatial attention at each layer. On the other hand, there are lines of work that fully fine-tune CLIP with minimal architectural modifications [5, 9, 26, 33]. ViFi-CLIP [26], a simple fine-tuning method with CLIP without additional temporal modules, generalizes well in open-vocabulary learning. Open-VCLIP [33] expands the temporal view of self-attention by adding keys and values of neighboring frames. Despite the generalization capacity of recent models, we argue they did not adequately leverage temporal information during the video feature encoding process, as they either rely on averaging frame-wise representations [26], [CLS] token interactions [22, 32], or considering only consecutive frames [33]. Unlike prior approaches, we explore a temporal information infusion method to ensure spatio-temporal representation modeling in a broader range.

Token aggregation. Conventional token aggregation methods, prioritizing efficiency enhancement, categorize into hard and soft clusterings. In hard clustering methods like K-Means [21], K-Medoids [15], and DPC-KNN [12], clusters are distinct without overlap, and every data point is assigned solely to one cluster. Bipartite matching [14] divides the data points into two groups and merges a specific number of edges with the highest scores. Soft clustering allows each data point to belong to multiple clusters with varying likelihood. Fuzzy C-Means [7] extends K-Means by enabling non-exclusive partitions and prototypes. Recent token aggregation methods for efficient ViTs [1, 19, 25, 29, 35] leverage aggregation algorithms to reduce the number of tokens for efficiency. While previous approaches focus on efficiency, we employ token aggregation approaches to link relevant tokens across the videos for contextual information.

Prompt learning. Many works have proposed to transfer VLMs to downstream tasks by optimizing a discrete set of prompt vectors [11, 13, 17, 26, 32, 37, 38]. In video recognition, [13] has introduced text prompt tuning, while ViFi-CLIP [26] and Vita-CLIP [32] perform prompting in both vision and text branches. However, these prompt vectors are individually optimized and not shared across the modalities. In image recognition, Co-CoOp [37] performs an instance-conditional prompt tuning by explicitly conditioning the text prompts on [CLS] tokens from image instances. MaPLe [17] learns multi-modal prompting by sharing layer-wise context prompts for both branches. Unlikely, we generate video-conditional prompts by utilizing contextualized tokens as vision inputs and injecting summarized video information into text prompt vectors.

3 Proposed Method

3.1 Preliminary

We first review how CLIP [24] is used for video action recognition. In particular, we discuss the encoding procedure based on the vision and text encoders of CLIP, denoted by $\{f_{\theta_v}, f_{\theta_c}\}$, to obtain video and text features, $\{\mathbf{v}, \mathbf{c}\}$.

Video encoding. Given a video $V \in \mathbb{R}^{T \times H \times W \times 3}$ of spatial resolution $H \times W$ with T sampled frames, following the Vision Transformer (ViT) architecture [6], we first divide each frame into $P \times P$ non-overlapping patches and flattening them as a set of vectors $\{\mathbf{x}_{t,i} \in \mathbb{R}^{3P^2}\}_{i=1}^N$, where t is the frame index, i is the patch index, and $N = HW/P^2$ is the number of patches. A sequence of tokens in the t^{th} frame, denoted by \mathbf{z}_t^0 , is fed into the CLIP vision encoder after combining with the spatial positional encoding \mathbf{e}_{pos} as

$$\mathbf{z}_t^0 = [\mathbf{x}_{\text{cls}}, \mathbf{x}_{t,1} \mathbf{W}_{\text{emb}}, \mathbf{x}_{t,2} \mathbf{W}_{\text{emb}}, \dots, \mathbf{x}_{t,N} \mathbf{W}_{\text{emb}}] + \mathbf{e}_{\text{pos}}, \quad (1)$$

where $\mathbf{x}_{\text{cls}} \in \mathbb{R}^{d_v}$ is a learnable classification embedding, [CLS] token, and $\mathbf{W}_{\text{emb}} \in \mathbb{R}^{3P^2 \times d_v}$ is a linear projection matrix. The CLIP vision encoder, $f_{\theta_v}(\cdot)$, sequentially encodes the frame-level representation \mathbf{z}_t^l at each layer $l \in \{1, \dots, L_v\}$ as follows:

$$\mathbf{z}_t^l = f_{\theta_v}^l(\mathbf{z}_t^{l-1}), \quad (2)$$

where $f_{\theta_v}^l(\cdot)$ is the l^{th} layer of the CLIP vision encoder. Then, we project the [CLS] token of the t^{th} frame, $\mathbf{z}_{t,0}^{L_v}$, onto a common vision-language latent space:

$$\mathbf{v}_t = \mathbf{z}_{t,0}^{L_v} \mathbf{W}_{\text{vis}}, \quad (3)$$

where $\mathbf{W}_{\text{vis}} \in \mathbb{R}^{d_v \times d_{v_l}}$ is a projection matrix. Finally, the video representation \mathbf{v} is obtained by averaging the per-frame representations \mathbf{v}_t as

$$\mathbf{v} = \text{AvgPool}([\mathbf{v}_1, \dots, \mathbf{v}_T]). \quad (4)$$

Text encoding. Given a text description C for a video, the input of the text encoder, \mathbf{c}^0 , is obtained by tokenizing words in the description and computing their word embedding vectors. In addition to the embeddings from category names, one can augment a sequence of prompt embeddings \mathbf{p}^0 , which are obtained from either hand-crafted templates such as “a photo of a” or learnable prompt vectors. The CLIP text encoder, $f_{\theta_c}(\cdot)$, sequentially processes a sequence of text embeddings including prompt embeddings, which is denoted by $[\mathbf{p}^0, \mathbf{c}^0]$, and computes an intermediate representation at each layer $l \in \{1, \dots, L_c\}$ as follows:

$$[\mathbf{p}^l, \mathbf{c}^l] = f_{\theta_c}^l([\mathbf{p}^{l-1}, \mathbf{c}^{l-1}]), \quad (5)$$

where $f_{\theta_c}^l(\cdot)$ denotes the l^{th} layer of the CLIP text encoder. The final text representations \mathbf{c} is obtained by projecting the [EOS] token from the last layer to the vision-language latent space using a matrix $\mathbf{W}_{\text{text}} \in \mathbb{R}^{d_l \times d_{v_l}}$, *i.e.*, $\mathbf{c} = \mathbf{c}_{\text{eos}}^{L_c} \mathbf{W}_{\text{text}}$.

Video-text alignment. Finally, the similarity between video and text embeddings are formulated as follows:

$$\text{sim}(\mathbf{v}, \mathbf{c}) = \frac{\langle \mathbf{v}, \mathbf{c} \rangle}{\|\mathbf{v}\| \|\mathbf{c}\|}. \quad (6)$$

During training, the goal is to maximize the similarity if V and C are matched but minimize it otherwise. For inference, the category with the highest similarity is chosen as the prediction output.

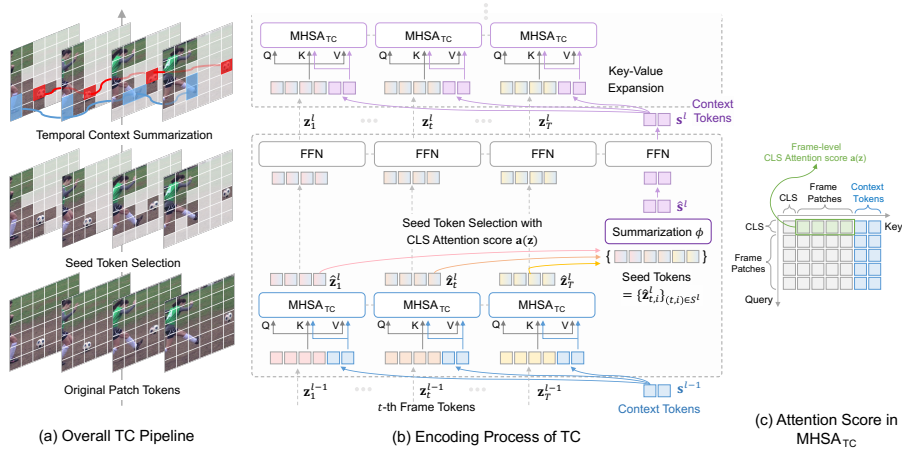


Fig. 4: Overview of Temporal Contextualization (TC). (a) Starting with the original patch tokens of the entire video, we first select informative seed tokens from each frame and perform temporal context summarization to aggregate relevant tokens to obtain context tokens. (b) The encoded context tokens are subsequently utilized as key-value pairs for self-attention in the next layer. (c) We employ attention score with [CLS] tokens as the criterion for seed token selection.

3.2 Temporal Contextualization (TC)

To alleviate the chronic drawbacks of existing CLIP-based video representations and leverage the spatio-temporal context in an entire video during the encoding process, we propose Temporal Contextualization (TC). TC consists of three steps, which are 1) informative token selection in each frame, 2) context summarization across spatio-temporal dimensions, and 3) temporal context infusion to all tokens in the subsequent layer. Fig. 4 illustrates an overview of TC. We discuss the three steps of our TC pipeline in the following.

Informative token selection. Due to a large number of redundant patches, the use of all patches for encoding a video may be suboptimal for extracting desired temporal information. Our approach focuses on selecting the informative tokens before performing the token aggregation. To this end, the attention scores obtained from self-attention operations in each frame are used as criteria to select seed tokens. Specifically, given patch tokens $\{z_{t,i}\}_{i=1}^N$ in the t^{th} frame, a set of attention scores $\{a(z_{t,i})\}_{i=1}^N$ is driven from the attention of the query of the [CLS] token to the keys of patch tokens, which is given by

$$\mathbf{a}(z_t) = \text{Softmax}\left(\frac{\mathbf{q}_{\text{cls}}\mathbf{K}_{z_t}^T}{\sqrt{d}}\right), \quad (7)$$

where both the query $\mathbf{q}_{\text{cls}} = z_{t,0}\mathbf{W}_q \in \mathbb{R}^d$ and keys $\mathbf{K}_{z_t} = z_t\mathbf{W}_k \in \mathbb{R}^{(N+1) \times d}$ are given by linear projections of input $z_t \in \mathbb{R}^{(N+1) \times d}$. In practice, our model yields multiple [CLS] attention scores through multi-head self-attention (MHSA) operations and compute the average of the attention scores from all heads, *i.e.*,

$\bar{\mathbf{a}}_{t,i} = \sum_{h=1}^H \mathbf{a}_{t,i}^h / H$, where $\mathbf{a}_{t,i}^h = \mathbf{a}^h(\mathbf{z}_{t,i})$ is the attention score for the i^{th} patch $\mathbf{z}_{t,i}$ in the t^{th} frame and H is a number of heads. Finally, we formulate a set of seed tokens for the t^{th} frame, \mathcal{S}_t , by selecting the indices for n_s elements with highest attention score $\bar{\mathbf{a}}_{t,i}$, where the number of seed tokens in each frame n_s is controlled by the ratio of $\alpha = n_s/N$.

Temporal context summarization. We now interconnect the seed tokens derived from individual frames based on their relevance and identify a collection of context tokens. Specifically, we collect all the seed tokens from all frames as $\mathcal{S} = \{(t, i) | i \in \mathcal{S}_t, t = 1, \dots, T\}$ and perform their spatio-temporal summarization by clustering and merging all the seed tokens in \mathcal{S} as follows:

$$\hat{\mathbf{s}} = \phi(\{\hat{\mathbf{z}}_{t,i}\}_{(t,i) \in \mathcal{S}}). \quad (8)$$

where $\hat{\mathbf{s}} \in \mathbb{R}^{k \times D}$ denotes a collection of the summarized tokens, which we call context tokens, ϕ is a token aggregation function, and $\hat{\mathbf{z}}_{t,i}$ indicates an interim token encoded from $\mathbf{z}_{t,i}$ via the self-attention operation. In practical, we construct a bipartite graph whose vertices and edges represent the original seed tokens and their pairwise similarities. Then, we iteratively perform bipartite matching [14] that splits the vertex set and merges r pairs of vertices based on their similarities by simple averaging of vertex features until there remain k number of tokens. Subsequently, the context tokens $\hat{\mathbf{s}}$ are fed into a feed-forward network (FFN) as done in the original encoding procedure and are forwarded to the next layer.

Temporal context infusion. Finally, we infuse the summarized context to all patch tokens by modifying the self-attention function. The keys and values of self-attention in every frame are expanded to include context tokens as follows:

$$\text{Attention}_{\text{TC}}(\mathbf{z}_t, \mathbf{s}) = \text{Softmax}\left(\frac{\mathbf{Q}_{\mathbf{z}_t} [\mathbf{K}_{\mathbf{z}_t} | \mathbf{K}_{\mathbf{s}}]^\top}{\sqrt{d}} + \mathbf{B}\right) [\mathbf{V}_{\mathbf{z}_t} | \mathbf{V}_{\mathbf{s}}], \quad (9)$$

where $\mathbf{K}_{\mathbf{s}} = \mathbf{s} \mathbf{W}_k$ and $\mathbf{V}_{\mathbf{s}} = \mathbf{s} \mathbf{W}_v$ are linear projections of the context tokens $\mathbf{s} \in \mathbb{R}^{k \times d}$. Here, $\mathbf{B} \in \mathbb{R}^{(N+1) \times (N+k+1)}$ is a bias matrix that distinguishes between frame-level local information and video-level global information in the expanded key matrix as

$$\mathbf{B}_{ij} = \begin{cases} b_{\text{local}} & \text{if } j \leq N + 1 \\ b_{\text{global}} & \text{otherwise,} \end{cases} \quad (10)$$

where b_{local} and b_{global} are learnable parameters and defined for multiple heads at each layer. We build our TC pipeline in a layer-wise manner, and thus the encoding process of each layer is expressed as

$$\hat{\mathbf{z}}_t^l = \begin{cases} \text{MHSA}(\text{LN}(\mathbf{z}_t^{l-1})) + \mathbf{z}_t^{l-1} & \text{if } l = 1 \\ \text{MHSA}_{\text{TC}}(\text{LN}(\mathbf{z}_t^{l-1}), \text{LN}(\mathbf{s}^{l-1})) + \mathbf{z}_t^{l-1} & \text{otherwise,} \end{cases} \quad (11)$$

$$\mathbf{z}_t^l = \text{FFN}(\text{LN}(\hat{\mathbf{z}}_t^l)) + \hat{\mathbf{z}}_t^l, \quad (12)$$

$$\mathbf{s}^l = \text{FFN}(\text{LN}(\hat{\mathbf{s}}^l)) + \hat{\mathbf{s}}^l, \quad (13)$$

where $\text{MHSA}_{\text{TC}}(\cdot, \cdot)$ denotes the TC-based MHSA operation including Eq. (9) and $\text{LN}(\cdot)$ stands for the layer normalization function.

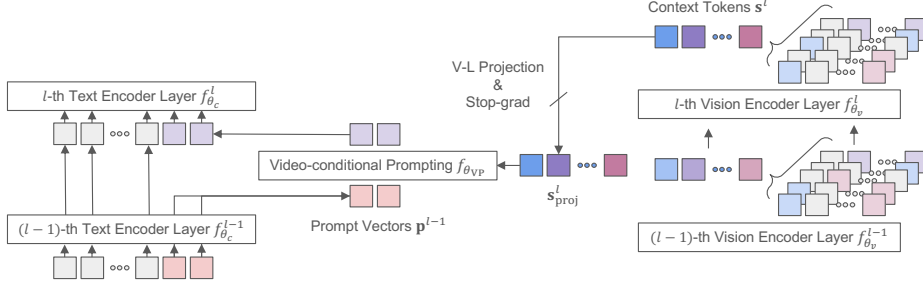


Fig. 5: Video-conditional Prompting (VP) module. Video information from the context tokens is injected to the text prompt vectors based on a cross-attention mechanism, generating instance-level prompts that support the lack of textual semantics.

3.3 Video-conditional Prompting (VP)

We present the Video-conditional Prompting (VP) module, which aims to further leverage the precisely aggregated temporal information in visual domain for text encoding. We impose a cross-attention between prompt vectors and context tokens to enrich the information in the prompt vectors, and the detailed procedure is illustrated in Fig. 5. Let \mathbf{c}^{l-1} and \mathbf{p}^{l-1} be class name tokens and learnable prompt vectors from the $(l-1)$ th layer of the text encoder, respectively. We derive temporally contextualized prompt vectors $\hat{\mathbf{p}}^{l-1}$ by passing the layer-normalized prompt tokens and context tokens through a cross-attention layer as follows:

$$\mathbf{s}_{\text{proj}}^l = \text{SG}(\mathbf{s}^l \mathbf{W}_{\text{vis}}), \quad (14)$$

$$\hat{\mathbf{p}}^{l-1} = \text{MHCA}(\text{LN}_p(\mathbf{p}^{l-1}), \text{LN}_s(\mathbf{s}_{\text{proj}}^l)) + \mathbf{p}^{l-1} \quad (15)$$

where $\text{SG}(\cdot)$ is a stop-gradient function, \mathbf{W}_{vis} is a weight matrix of CLIP to linearly project vision representations to a common vision-language latent space, and $\text{MHCA}(\cdot, \cdot)$ is a multi-head cross-attention operation for interactions across modalities, accepting text prompt vectors as queries and vision features as keys and values. Finally, the contextualized prompt vector $\hat{\mathbf{p}}^{l-1}$ are updated by FFN:

$$\tilde{\mathbf{p}}^{l-1} = \text{FFN}(\text{LN}(\hat{\mathbf{p}}^{l-1}) + \hat{\mathbf{p}}^{l-1}) \quad (16)$$

The VP module $f_{\theta_{\text{VP}}}(\cdot, \cdot)$ is defined by a composition of Eq. (15) and Eq. (16), and executed before the last layer of text encoder f_{θ_c} . Finally, the new formulation of our encoding process in the text modality is given by

$$[\mathbf{p}^l, \mathbf{c}^l] = \begin{cases} f_{\theta_c}^l([f_{\theta_{\text{VP}}}(\tilde{\mathbf{p}}^{l-1}, \mathbf{s}_{\text{proj}}^l), \mathbf{c}^{l-1}]) & \text{if } l = L_c \\ f_{\theta_c}^l([\mathbf{p}^{l-1}, \mathbf{c}^{l-1}]) & \text{otherwise.} \end{cases} \quad (17)$$

The resulting instance-conditioned prompt vectors effectively support the lack of textual semantics in action recognition datasets. The impact of our VP design is verified in the experiments in Sec. 5.

3.4 Training Objective

TC-CLIP learns to maximize the similarity of video representations \mathbf{v} and text representations \mathbf{c} for matching pairs in a mini-batch via the cross-entropy loss:

$$\mathcal{L} = - \sum_i \log \frac{\exp(\text{sim}(\mathbf{v}_i, \mathbf{c}_i)/\tau)}{\sum_j \exp(\text{sim}(\mathbf{v}_i, \mathbf{c}_j)/\tau)}, \quad (18)$$

where τ is a learnable temperature parameter. Our model is fully fine-tuned in an end-to-end manner.

4 Experiments

4.1 Experimental Setup

Datasets. We conduct experiments over 5 video benchmarks: Kinetics-400 [16] & 600 [2], HMDB-51 [18], UCF-101 [28], and Something-Something v2 (SSv2) [8]. Following [26], our evaluation protocol includes zero-shot, few-shot, base-to-novel generalization, and fully-supervised action recognition.

Implementation details. We adopt CLIP with ViT-B/16 for all experiments. Our baseline is ViFi-CLIP [26]. During the training, we sample 16 frames to form a video clip. During the evaluation, two temporal clips with one spatial crop (2×1 view) per video are sampled to produce a prediction unless otherwise stated. For training recipes, we follow [26] for zero-shot, few-shot, and fully-supervised settings and follow [9] for base-to-novel generalization. Following [5, 9, 20, 33], we adopt linear weight-space ensembling of our fine-tuned model and CLIP for the zero-shot protocol. We set the number of merged tokens r in each bipartite matching iteration to 100, and the weight of the VP module is initialized with the weight from the last layer of the CLIP text encoder. All models are trained using 4 NVIDIA Tesla V100 GPUs. See supplementary material for more details.

4.2 Quantitative Comparison

We mainly compare our method with CLIP-based video recognition models: Vanilla CLIP [24], ActionCLIP [30], A5 [13], X-CLIP [22], Vita-CLIP [32], ViFi-CLIP [26], Open-VCLIP [33], OST [5], and FROSTER [9]. To fairly compare our method with approaches that utilize Large Language Model (LLM)-based text augmentation [5, 9, 20], we divide our results into two versions: one using the original action category names (colored with `blue`) and the other adopting the LLM-rephrased category names from FROSTER [9] (colored with `purple`). Note that experiments on the SSv2 dataset do not involve LLM-rephrasing.

Zero-shot action recognition. We assess the generalization ability of our method in the zero-shot video action recognition. We train CLIP on K-400 and evaluate the zero-shot classification accuracy on HMDB-51, UCF-101, and K-600. As shown in Table 1, our TC-CLIP achieves an average accuracy of 71.0%,

Table 1: Comparison with state-of-the-arts on zero-shot action recognition. All the models are trained on Kinetics-400 and directly evaluated on other datasets. † denotes the methods with weight-space ensemble. Our results using the original and LLM-rephrased category names are highlighted in blue and purple, respectively.

Method	HMDB-51	UCF-101	K600 (Top-1)	K600 (Top-5)	All (Top-1)
Vanilla CLIP [24]	40.8 ± 0.3	63.2 ± 0.2	59.8 ± 0.3	83.5 ± 0.2	54.6
ActionCLIP [30]	40.8 ± 5.4	58.3 ± 3.4	66.7 ± 1.1	91.6 ± 0.3	55.3
A5 [13]	44.3 ± 2.2	69.3 ± 4.2	55.8 ± 0.7	81.4 ± 0.3	56.5
X-CLIP [22]	44.6 ± 5.2	72.0 ± 2.3	65.2 ± 0.4	86.1 ± 0.8	60.6
Vita-CLIP [32]	48.6 ± 0.6	75.0 ± 0.6	67.4 ± 0.5	-	63.7
ViFi-CLIP [26]	51.3 ± 0.6	76.8 ± 0.7	71.2 ± 1.0	92.2 ± 0.3	66.4
Open-VCLIP [33] †	53.9 ± 1.2	83.4 ± 1.2	73.0 ± 0.8	93.2 ± 0.1	70.1
TC-CLIP (Ours) †	54.2 ± 0.7	82.9 ± 0.6	75.8 ± 0.5	94.4 ± 0.2	71.0
<i>Using LLM-based text augmentation</i>					
MAXI [20] †	52.3 ± 0.7	78.2 ± 0.8	71.5 ± 0.8	92.5 ± 0.4	67.3
OST [5] †	55.9 ± 1.2	79.7 ± 1.1	75.1 ± 0.6	94.6 ± 0.2	70.2
FROSTER [9] †	54.8 ± 1.3	84.8 ± 1.1	74.8 ± 0.9	-	71.5
TC-CLIP (Ours) †	56.0 ± 0.3	85.4 ± 0.8	78.1 ± 1.0	95.7 ± 0.3	73.2

Table 2: Comparison with state-of-the-arts on few-shot action recognition. All the models are directly fine-tuned from CLIP. Our results using the original and LLM-rephrased category names are highlighted in blue and purple, respectively.

Method	HMDB-51				UCF-101				SSv2				All
	K=2	K=4	K=8	K=16	K=2	K=4	K=8	K=16	K=2	K=4	K=8	K=16	
Vanilla CLIP [24]	41.9	41.9	41.9	41.9	63.6	63.6	63.6	63.6	2.7	2.7	2.7	2.7	36.1
ActionCLIP [30]	47.5	57.9	57.3	59.1	70.6	71.5	73.0	91.4	4.1	5.8	8.4	11.1	46.5
A5 [13]	39.7	50.7	56.0	62.4	71.4	79.9	85.7	89.9	4.4	5.1	6.1	9.7	46.8
X-CLIP [22]	53.0	57.3	62.8	64.0	76.4	83.4	88.3	91.4	3.9	4.5	6.8	10.0	50.2
ViFi-CLIP [26]	57.2	62.7	64.5	66.8	80.7	85.1	90.0	92.7	6.2	7.4	8.5	12.4	52.9
TC-CLIP (Ours)	57.3	62.3	67.3	68.6	85.9	89.9	92.5	94.6	7.3	8.6	9.3	14.0	54.8
<i>Using LLM-based text augmentation</i>													
OST [5]	59.1	62.9	64.9	68.2	82.5	87.5	91.7	93.9	7.0	7.7	8.9	12.2	53.9
TC-CLIP (Ours)	58.6	63.3	65.5	68.8	86.8	90.1	92.0	94.3	7.3	8.6	9.3	14.0	54.9

exhibiting significant gaps of at least 0.9%p compared to state-of-the-art video action recognition methods. The utilization of LLM-based text augmentation further enhances the classification accuracy by 2.2%p, surpassing other methods by 1.7%p. Moreover, our method consistently outperforms others across all datasets. These results posit the superior generalization ability of our method.

Few-shot action recognition. We demonstrate the learning capacity of our method under a challenging few-shot scenario. In this setting, models are directly fine-tuned from CLIP on HMDB-51, UCF-101, and SSv2 using K -shot samples, where K is set to 2, 4, 8, and 16. Table 2 shows the comparison with state-of-the-art video action recognition methods on the few-shot setting. Our method achieves state-of-the-art performance with an average accuracy of 54.8%, surpassing our baseline model ViFi-CLIP [26] by 1.9%p.

Base-to-novel generalization. Similar to the few-shot setting, models are directly fine-tuned from CLIP on the base classes of K-400, HMDB-51, UCF-101, and SSv2, and evaluated for both base and novel classes. The top-1 accuracy

Table 3: Comparison with state-of-the-arts on base-to-novel generalization. All the models are directly fine-tuned from CLIP. † denotes the results are taken from [9]. Our results using the original and LLM-rephrased category names are highlighted in blue and purple, respectively.

Method	K-400			HMDB-51			UCF-101			SSv2			All (Avg.)		
	Base	Novel	HM	Base	Novel	HM	Base	Novel	HM	Base	Novel	HM	Base	Novel	HM
Vanilla CLIP [24]	62.3	53.4	57.5	53.3	46.8	49.8	78.5	63.6	70.3	4.9	5.3	5.1	49.8	42.3	45.7
ActionCLIP [30]	61.0	46.2	52.6	69.1	37.3	48.5	90.1	58.1	70.7	13.3	10.1	11.5	58.5	37.9	46.0
A5 [13]	69.7	37.6	48.8	46.2	16.0	23.8	90.5	40.4	55.8	8.3	5.3	6.4	53.7	24.8	33.9
X-CLIP [22]	74.1	56.4	64.0	69.4	45.5	55.0	89.9	58.9	71.2	8.5	6.6	7.4	60.5	41.9	49.5
ViFi-CLIP [26]	76.4	61.1	67.9	73.8	53.3	61.9	92.9	67.7	78.3	16.2	12.1	13.9	64.8	48.6	55.5
Open-VCLIP [33] †	76.5	62.6	68.9	70.3	50.4	58.9	94.8	77.5	85.3	16.0	11.0	13.0	64.4	50.4	56.5
TC-CLIP (Ours)	78.9	63.6	70.4	73.3	54.1	62.2	95.5	78.0	85.9	17.5	13.4	15.2	66.3	52.3	58.5

Using LLM-based text augmentation

FROSTER [9]	77.8	64.3	70.4	74.1	58.0	65.1	95.3	80.0	87.0	18.3	12.2	14.6	66.4	53.6	59.3
TC-CLIP (Ours)	79.1	65.4	71.6	73.3	59.1	65.5	95.4	81.6	88.0	17.5	13.4	15.2	66.3	54.9	60.1

Table 4: Comparison with state-of-the-arts on fully-supervised action recognition on Kinetics-400. Views are denoted with temporal clips \times spatial crops. † means that computational costs are measured in our environment using a single V100 GPU. The results of other methods are taken from [26].

Method	Top-1	Top-5	Frames	Views	GFLOPs	Params (M)
ActionCLIP [30]	83.8	96.2	32	10 \times 3	563	168.5
X-CLIP [22]	84.7	96.8	16	4 \times 3	287	131.5
Vita-CLIP [22] †	82.9	96.3	16	4 \times 3	307	185.3
ViFi-CLIP [26]	83.9	96.3	16	4 \times 3	281	124.7
OST [5]	83.2	-	16	1 \times 1	-	-
TC-CLIP (Ours)	85.2	96.9	16	4 \times 3	304	127.5

on base and novel classes, and their harmonic mean (HM) are reported. Table 3 shows that our model achieves state-of-the-art performance on the novel classes and HM across all datasets. In particular, TC-CLIP achieves an average HM accuracy of 58.5%, surpassing previous state-of-the-arts by 2.0%p.

Fully-supervised action recognition. Table 4 shows performance comparison results under fully-supervised setting, where the models are both trained and evaluated on the K-400 dataset. Our model achieves top-1 accuracy of 85.2% in the K-400 validation split, improving 1.3%p over our baseline ViFi-CLIP [26].

5 Analysis and Discussion

This section examines the design choices and impact of each component in our model: Temporal Contextualization (TC) and Video-conditional Prompting (VP). We mainly adopt the zero- and few-shot settings and report the average of top-1 accuracy from $K = 2, 4, 8, 16$ for the K -shot setup.

5.1 Component-wise Ablation

Table 5 shows the impact of TC, VP, and weight-space ensembling (WE) on our baseline in the zero-shot setting. (a) Adopting TC with WE leads to an

Table 5: Component-wise ablation on the zero-shot setting. (Δ) denotes the average top-1 accuracy improvement over baseline.

Case	TC	VP	WE	HMDB-51	UCF-101	K-600	All (Δ)
Baseline				52.3 \pm 0.2	78.9 \pm 1.1	70.7 \pm 0.8	67.3
(a) w/o Video-conditional Prompting (VP)	✓		✓	54.3 \pm 0.6	81.9 \pm 1.0	75.5 \pm 0.5	70.6 (+3.3)
(b) w/o Temporal Contextualization (TC)		✓	✓	53.2 \pm 0.8	82.0 \pm 0.9	74.7 \pm 0.7	70.0 (+2.7)
(c) w/o Weight-space Ensembling (WE)	✓	✓		53.7 \pm 0.7	80.4 \pm 0.9	72.7 \pm 0.5	68.9 (+1.6)
TC-CLIP	✓	✓	✓	54.2 \pm 0.7	82.9 \pm 0.6	75.8 \pm 0.5	71.0 (+3.7)

Table 6: Temporal Contextualization (TC) ablation on the few-shot setting. SE, JE, and Bias denote spatial embedding, joint space-time embedding, and bias (Eq. 10). Default settings are marked in gray.

(a) Seed token selection metric.					(b) Token aggregation method.									
Case	HMDB	UCF	SSv2	All	Case	HMDB	UCF	SSv2	All					
No selection	62.8	89.8	9.7	54.1	No merge	57.2	85.6	7.7	50.2					
Head-wise key norm	62.3	89.8	9.8	54.0	Temporal tube	57.9	86.4	8.3	50.9					
Averaged key norm	62.5	89.4	9.3	53.7	Random merge	58.8	87.1	7.5	51.2					
Head-wise CLS attention	63.4	89.9	9.7	54.3	K-means	61.7	89.7	9.0	53.4					
Averaged CLS attention	63.4	90.2	9.9	54.5	Bipartite matching	63.4	90.2	9.9	54.5					
(c) Seed token ratio α .					(d) Context token k .					(e) Positional embedding.				
α	HMDB	UCF	SSv2	All	k	HMDB	UCF	SSv2	All	Case	HMDB	UCF	SSv2	All
0.2	62.6	90.1	9.8	54.2	16	63.1	89.3	9.1	53.8	SE	62.9	90.0	9.8	54.2
0.3	63.4	90.2	9.9	54.5	32	63.6	89.9	9.4	54.3	JE	63.2	90.2	9.8	54.4
0.4	63.2	90.4	9.8	54.5	64	63.7	90.1	9.7	54.5	SE+Bias	63.4	90.2	9.9	54.5
0.5	63.3	90.3	9.8	54.5	96	63.4	90.2	9.9	54.5	JE+Bias	62.9	90.2	9.8	54.3
0.6	63.1	90.2	9.8	54.4	128	62.8	90.1	9.9	54.3					
					256	60.9	89.5	9.3	53.2					

average gain of 3.3%p, while (b) incorporating VP with WE results in a 2.7%p improvement, highlighting the significance of TC in our framework. (c) When both VP and TC are applied to the baseline, we observed a 1.6%p improvement on average. Finally, by integrating all three components, TC-CLIP achieves a total 3.7%p gain on average.

5.2 Temporal Contextualization (TC) Ablation

Table 6 analyzes the design choice of TC. Experiments are conducted on the few-shot setting using the baseline model with TC.

Seed token selection metric. Using [CLS] attention score averaged from multiple heads is the best choice, resulting in a 0.4%p gain on average compared to the no-selection case, *i.e.*, using all tokens for aggregation.

Token aggregation methods. Using seed tokens without merging leads to inferior performance, encountering the extrapolation issue. When comparing naive aggregation methods, random merge surpasses temporal tube since random merge has more chance to aggregate relevant tokens while temporal tube are enforced to group tokens of the same spatial positions. Finally, we compared the clustering algorithms and selected bipartite matching as our default choice.

Seed token selection ratio α . While TC is not sensitive to the choice of α , we picked $\alpha = 0.3$ as our default value, *i.e.*, using 30% of total tokens.

Table 7: Video-conditional Prompting (VP) ablation. Default settings are marked in gray .

(a) Vision token selection (few-shot).					(b) Number of prompt vectors (few-shot).				
Case	HMDB	UCF	SSv2	All	Case	HMDB	UCF	SSv2	All
CLS tokens	63.3	90.3	9.8	54.4	2	62.0	90.1	9.4	53.8
GAP tokens	63.7	90.5	9.8	54.7	4	63.9	90.7	9.8	54.8
Context tokens	63.9	90.7	9.8	54.8	8	63.7	90.4	9.8	54.7

(c) Text prompting design (zero-shot). All the models are evaluated without weight ensembling.					
Case	Use context tokens?	HMDB-51	UCF-101	K-600	All (Δ)
Baseline		52.3 \pm 0.2	78.9 \pm 1.1	70.7 \pm 0.8	67.3
(a) Learnable prompt vectors		52.4 \pm 0.4	78.4 \pm 1.3	70.6 \pm 0.7	67.1 (-0.2)
(b) Video-conditional prompting		53.2 \pm 0.8	80.4 \pm 0.7	71.6 \pm 0.9	68.4 (+1.1)
(c) Video-conditional prompting	✓	53.7 \pm 0.7	80.4 \pm 0.9	72.7 \pm 0.5	68.9 (+1.6)
(d) Vision-text late-fusion	✓	53.7 \pm 0.7	79.0 \pm 0.7	70.9 \pm 0.6	67.9 (+0.6)

Context token number k . By varying the value of k , we observed that selecting a modest amount of merging degree is important for achieving the best performance. An excessively low k leads to the lost of spatial details like part-wise information, while an overly high k results in inadequate contextualization of tokens into relevant sets. Therefore, we choose $k = 96$ as our default setting.

Positional embedding. Among spatial embedding (SE), joint space-time embedding (JE), and our proposed learnable bias (Eq. 10), we observe that using SE with bias yields the best result. We conjecture that the bias effectively consolidates the local frame-level information and global video-level information in a layer-wise and head-wise manner.

5.3 Video-conditional Prompting (VP) Ablation

In Table 7, we analyze the design choice of the VP module in TC-CLIP on the few-shot and zero-shot setting.

Vision token selection. We compare using the context tokens with using [CLS] or Global Average Pooled (GAP) tokens from every frame. Using context tokens yields the best result, demonstrating that the proper contextualization from the video is essential for transferring the video information to the text side.

Number of prompt vectors. Increasing the number of prompt vectors does not necessarily improve performance. 4 prompt vectors are employed by default.

Text prompting design. We observe that (a) naively adding learnable prompt vectors without video instance conditioning does not enhance the zero-shot transferability and decreases the average accuracy by 0.2%p. (b) In contrast, employing VP design with [CLS] tokens consistently improves the accuracy across all datasets, and (c) using context tokens further enhances the performance, resulting in a 1.6%p gain. We also compare VP with (d) vision-text late-fusion design, *i.e.*, the cross-attention of context tokens and the final representation of the text embedding. This design shows worse performance in UCF-101 and K-600 datasets than our VP, demonstrating the superiority of our design choice.

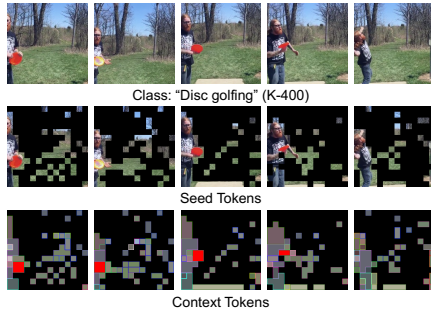


Fig. 6: Context token visualization. TC-CLIP selects the informative seed tokens and summarizes them into context tokens across frames. The disc (red) is merged into one token over the video.

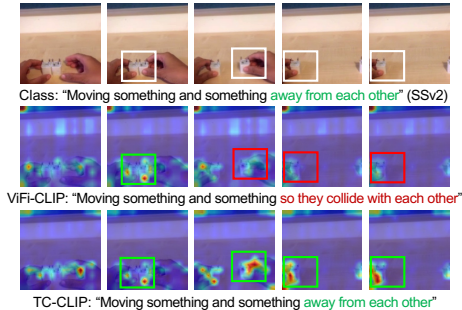


Fig. 7: Attention visualization. While ViFi-CLIP fails to attend to the movement of hands moving farther away and misinterprets the action as colliding, TC-CLIP correctly predicts with temporal consistency.

5.4 Qualitative Analysis

Context token visualization. Fig. 6 visualizes the seed tokens and context tokens from the last layer of the vision encoder in TC-CLIP. In this video, the informative regions regarding the action of “disc golfing” in each frame, including the person and the disc, are selected as seed tokens. To visualize each context token, we colorize its corresponding source token positions using the average color of the input image patches of that region. Note that a single context token (highlighted in red) successfully tracks the disc across multiple frames.

Attention visualization. Fig. 7 visualizes the attention map of ViFi-CLIP [26] and our TC-CLIP on the SSv2 dataset. In this video where two hands grab objects and then move away, ViFi-CLIP [26] fails to attend to the hands from the middle of the sequence and misinterprets the action as “colliding with each other”. In contrast, our TC-CLIP considers the temporal context across the sequence by its design, and thus consistently attends to the hands throughout the entire video and correctly predicts the action as “moving away from each other”. See more visualizations in Appendix E.

6 Conclusion

We have introduced TC-CLIP, a novel video understanding paradigm that leverages holistic video information within the encoding process. Unlike prior approaches that access only a limited range of tokens, our temporal contextualization summarizes informative tokens from the entire video and utilizes them during the attention operation. While these tokens are exploited to infuse temporal information on the vision side, they also serve as a source for video-conditional text prompting, enhancing instance-wise context on the text side. Extensive experiments and analysis on diverse video recognition benchmarks and evaluation protocols demonstrate the superiority of TC-CLIP and its design choices.

Limitation. Due to resource constraints, we verified TC-CLIP only using ViT-B. We will further explore its scalability with ViT-L and ViT-H.

References

1. Bolya, D., Fu, C.Y., Dai, X., Zhang, P., Feichtenhofer, C., Hoffman, J.: Token merging: Your vit but faster. arXiv preprint arXiv:2210.09461 (2022) [4](#)
2. Carreira, J., Noland, E., Banki-Horvath, A., Hillier, C., Zisserman, A.: A short note about kinetics-600. arXiv preprint arXiv:1808.01340 (2018) [3](#), [9](#), [23](#)
3. Chen, S., Huang, D.: Elaborative rehearsal for zero-shot action recognition. In: ICCV (2021) [24](#)
4. Chen, S., Wong, S., Chen, L., Tian, Y.: Extending context window of large language models via positional interpolation. arXiv preprint arXiv:2306.15595 (2023) [2](#)
5. Chen, T., Yu, H., Yang, Z., Li, Z., Sun, W., Chen, C.: Ost: Refining text knowledge with optimal spatio-temporal descriptor for general video recognition. arXiv preprint arXiv:2312.00096 (2023) [1](#), [3](#), [4](#), [9](#), [10](#), [11](#)
6. Dosovitskiy, A., Beyer, L., Kolesnikov, A., Weissenborn, D., Zhai, X., Unterthiner, T., Dehghani, M., Minderer, M., Heigold, G., Gelly, S., et al.: An image is worth 16x16 words: Transformers for image recognition at scale. In: ICLR (2021) [5](#)
7. Ghosh, S., Dubey, S.K.: Comparative analysis of k-means and fuzzy c-means algorithms. International Journal of Advanced Computer Science and Applications **4**(4) (2013) [4](#)
8. Goyal, R., Ebrahimi Kahou, S., Michalski, V., Materzynska, J., Westphal, S., Kim, H., Haenel, V., Fruend, I., Yianilos, P., Mueller-Freitag, M., et al.: The "something something" video database for learning and evaluating visual common sense. In: ICCV (2017) [3](#), [9](#), [23](#)
9. Huang, X., Zhou, H., Yao, K., Han, K.: Froster: Frozen clip is a strong teacher for open-vocabulary action recognition. arXiv preprint arXiv:2402.03241 (2024) [1](#), [3](#), [4](#), [9](#), [10](#), [11](#), [24](#)
10. Jia, C., Yang, Y., Xia, Y., Chen, Y.T., Parekh, Z., Pham, H., Le, Q., Sung, Y.H., Li, Z., Duerig, T.: Scaling up visual and vision-language representation learning with noisy text supervision. In: ICML (2021) [1](#), [3](#)
11. Jia, M., Tang, L., Chen, B.C., Cardie, C., Belongie, S., Hariharan, B., Lim, S.N.: Visual prompt tuning. In: ECCV (2022) [4](#)
12. Jiang, J., Chen, Y., Meng, X., Wang, L., Li, K.: A novel density peaks clustering algorithm based on k nearest neighbors for improving assignment process. Physica A: Statistical Mechanics and its Applications **523**, 702–713 (2019) [4](#)
13. Ju, C., Han, T., Zheng, K., Zhang, Y., Xie, W.: Prompting visual-language models for efficient video understanding. In: ECCV (2022) [1](#), [3](#), [4](#), [9](#), [10](#), [11](#), [18](#)
14. Karp, R.M., Vazirani, U.V., Vazirani, V.V.: An optimal algorithm for on-line bipartite matching. In: Proceedings of the twenty-second annual ACM symposium on Theory of computing (1990) [4](#), [7](#)
15. Kaufman, L.: Partitioning around medoids (program pam). Finding groups in data **344**, 68–125 (1990) [4](#)
16. Kay, W., Carreira, J., Simonyan, K., Zhang, B., Hillier, C., Vijayanarasimhan, S., Viola, F., Green, T., Back, T., Natsev, P., et al.: The kinetics human action video dataset. arXiv preprint arXiv:1705.06950 (2017) [3](#), [9](#), [23](#)
17. Khattak, M.U., Rasheed, H., Maaz, M., Khan, S., Khan, F.S.: Maple: Multi-modal prompt learning. In: CVPR (2023) [4](#), [20](#), [23](#)

18. Kuehne, H., Jhuang, H., Garrote, E., Poggio, T., Serre, T.: Hmdb: a large video database for human motion recognition. In: ICCV (2011) [3](#), [9](#), [23](#)
19. Liang, Y., GE, C., Tong, Z., Song, Y., Wang, J., Xie, P.: EVit: Expediting vision transformers via token reorganizations. In: ICLR (2022) [4](#)
20. Lin, W., Karlinsky, L., Shvetsova, N., Possegger, H., Kozinski, M., Panda, R., Feris, R., Kuehne, H., Bischof, H.: Match, expand and improve: Unsupervised finetuning for zero-shot action recognition with language knowledge. In: ICCV (2023) [3](#), [9](#), [10](#)
21. Lloyd, S.: Least squares quantization in pcm. IEEE Transactions on Information Theory **28**(2), 129–137 (1982) [4](#)
22. Ni, B., Peng, H., Chen, M., Zhang, S., Meng, G., Fu, J., Xiang, S., Ling, H.: Expanding language-image pretrained models for general video recognition. In: ECCV (2022) [1](#), [2](#), [3](#), [4](#), [9](#), [10](#), [11](#), [18](#)
23. Press, O., Smith, N.A., Lewis, M.: Train short, test long: Attention with linear biases enables input length extrapolation. In: ICLR (2022) [2](#)
24. Radford, A., Kim, J.W., Hallacy, C., Ramesh, A., Goh, G., Agarwal, S., Sastry, G., Askell, A., Mishkin, P., Clark, J., et al.: Learning transferable visual models from natural language supervision. In: ICML (2021) [1](#), [3](#), [4](#), [9](#), [10](#), [11](#)
25. Rao, Y., Zhao, W., Liu, B., Lu, J., Zhou, J., Hsieh, C.J.: Dynamicvit: Efficient vision transformers with dynamic token sparsification. In: NeurIPS (2021) [4](#)
26. Rasheed, H., Khattak, M.U., Maaz, M., Khan, S., Khan, F.S.: Fine-tuned clip models are efficient video learners. In: CVPR (2023) [1](#), [3](#), [4](#), [9](#), [10](#), [11](#), [14](#), [18](#), [19](#), [20](#), [22](#), [23](#), [24](#)
27. Sevilla-Lara, L., Zha, S., Yan, Z., Goswami, V., Feiszli, M., Torresani, L.: Only time can tell: Discovering temporal data for temporal modeling. In: WACV (2021) [19](#)
28. Soomro, K., Zamir, A.R., Shah, M.: Ucf101: A dataset of 101 human actions classes from videos in the wild. arXiv preprint arXiv:1212.0402 (2012) [3](#), [9](#), [23](#)
29. Tang, Y., Han, K., Wang, Y., Xu, C., Guo, J., Xu, C., Tao, D.: Patch slimming for efficient vision transformers. In: CVPR (2022) [4](#)
30. Wang, M., Xing, J., Liu, Y.: Actionclip: A new paradigm for video action recognition. arXiv preprint arXiv:2109.08472 (2021) [1](#), [3](#), [9](#), [10](#), [11](#), [18](#)
31. Wang, Y., He, Y., Li, Y., Li, K., Yu, J., Ma, X., Li, X., Chen, G., Chen, X., Wang, Y., et al.: Internvid: A large-scale video-text dataset for multimodal understanding and generation. arXiv preprint arXiv:2307.06942 (2023) [1](#)
32. Wasim, S.T., Naseer, M., Khan, S., Khan, F.S., Shah, M.: Vita-clip: Video and text adaptive clip via multimodal prompting. In: CVPR (2023) [1](#), [2](#), [3](#), [4](#), [9](#), [10](#)
33. Weng, Z., Yang, X., Li, A., Wu, Z., Jiang, Y.G.: Open-vclip: Transforming clip to an open-vocabulary video model via interpolated weight optimization. In: ICML (2023) [1](#), [2](#), [3](#), [4](#), [9](#), [10](#), [11](#)
34. Xu, H., Ghosh, G., Huang, P.Y., Okhonko, D., Aghajanyan, A., Metze, F., Zettlemoyer, L., Feichtenhofer, C.: Videoclip: Contrastive pre-training for zero-shot video-text understanding. arXiv preprint arXiv:2109.14084 (2021) [1](#)
35. Xu, Y., Zhang, Z., Zhang, M., Sheng, K., Li, K., Dong, W., Zhang, L., Xu, C., Sun, X.: Evo-vit: Slow-fast token evolution for dynamic vision transformer. In: AAAI (2022) [4](#)
36. Yuan, L., Chen, D., Chen, Y.L., Codella, N., Dai, X., Gao, J., Hu, H., Huang, X., Li, B., Li, C., et al.: Florence: A new foundation model for computer vision. arXiv preprint arXiv:2111.11432 (2021) [1](#), [3](#)
37. Zhou, K., Yang, J., Loy, C.C., Liu, Z.: Conditional prompt learning for vision-language models. In: CVPR (2022) [4](#), [20](#), [23](#)

38. Zhou, K., Yang, J., Loy, C.C., Liu, Z.: Learning to prompt for vision-language models. *IJCV* (2022) [4](#)

Leveraging Temporal Contextualization for Video Action Recognition

——Supplementary Material——

We provide additional experimental analyses and details in the following order:

- Appendix **A**: Fine-tuning with the Kinetics-400 pretrained model
- Appendix **B**: Temporal subset analysis
- Appendix **C**: More ablation study on VP
- Appendix **D**: Impact of weight-space ensemble
- Appendix **E**: More visualizations of context tokens and attentions
- Appendix **F**: Datasets and implementation details

A Fine-tuning with the Kinetics-400 Pretrained Model

Table 8: Comparison with state-of-the-arts on few-shot action recognition using Kinetics-400 pretrained model. All the models are first pretrained on Kinetics-400 and subsequently fine-tuned on each dataset.

Method	HMDB-51				UCF-101				SSv2				All
	$K=2$	$K=4$	$K=8$	$K=16$	$K=2$	$K=4$	$K=8$	$K=16$	$K=2$	$K=4$	$K=8$	$K=16$	
ActionCLIP [30]	54.3	56.2	59.3	66.1	76.7	80.4	87.6	91.8	4.8	6.9	9.1	12.3	50.5
A5 [13]	46.7	50.4	61.3	65.8	76.3	84.4	90.7	93.0	4.5	6.7	7.2	9.5	49.7
X-CLIP [22]	60.5	66.8	69.3	71.7	89.0	91.4	94.7	96.3	6.6	7.8	9.9	13.7	56.5
ViFi-CLIP [26]	63.0	65.1	69.6	72.0	91.0	93.7	95.0	96.4	6.7	7.9	10.2	13.5	57.0
TC-CLIP (Ours)	65.3	68.5	71.4	73.0	94.1	95.6	96.6	97.3	8.7	10.1	12.1	15.2	59.0

Table 9: Comparison with state-of-the-arts on base-to-novel generalization using Kinetics-400 pretrained model. All the models are first pretrained on Kinetics-400 and subsequently fine-tuned on each dataset.

Method	HMDB-51			UCF-101			SSv2			All (Avg.)		
	Base	Novel	HM	Base	Novel	HM	Base	Novel	HM	Base	Novel	HM
ActionCLIP [30]	69.0	57.2	62.6	85.6	75.3	80.1	8.1	8.7	8.4	54.2	47.1	50.4
A5 [13]	70.4	51.7	59.6	95.8	71.0	81.6	12.9	5.7	7.9	59.7	42.8	49.9
X-CLIP [22]	75.8	52.0	61.7	95.4	74.0	83.4	14.2	11.0	12.4	61.8	45.7	52.5
ViFi-CLIP [26]	77.1	54.9	64.1	95.9	74.1	83.6	15.8	11.5	13.3	62.9	46.8	53.7
TC-CLIP (Ours)	79.4	58.3	67.2	97.5	84.5	90.5	19.6	15.6	17.4	65.5	52.8	58.5

We additionally compare TC-CLIP with the state-of-the-art methods on few-shot and base-to-novel settings using the Kinetics-400 pretrained model. In this setting, all the models are first pretrained on the Kinetics-400 dataset and subsequently fine-tuned on each dataset. Table 8 summarizes the comparison results in the few-shot action recognition regime. Notably, TC-CLIP surpasses other methods by a large margin of at least 2%p in the average. Furthermore, Table 9 shows the comparison results in the base-to-novel generalization setup. In an

Table 10: Temporal subset analysis using the temporal subset [27] on Kinetics-400 and SSv2. Gains over ViFi-CLIP are indicated in green.

Method	K-400 fully-supervised		SSv2 16-shot	
	All	Temporal	All	Temporal
ViFi-CLIP [26]	83.9	87.8	12.4	25.9
TC-CLIP (Ours)	85.2 (+1.3)	89.2 (+1.4)	14.0 (+1.6)	29.9 (+4.0)

Table 11: VP layer selection ablation. We report K -shot training results where the top-1 accuracy in each dataset is averaged over $K = 2, 4, 8, 16$. The late-stage prompting design generalizes well.

L_{text}	L_{vision}	HMDB	UCF	SSv2	All
1	1	62.3	89.7	9.1	53.7
1	12	62.0	89.9	9.3	53.7
6	6	62.8	89.5	9.7	54.0
6	12	62.5	90.2	9.7	54.1
12	12	63.9	90.7	9.8	54.8

Table 12: VP initialization ablation by varying initialization cases of the VP layer and prompt vectors. We report K -shot training results where the top-1 accuracy is averaged over $K = 2, 4, 8, 16$. In general, it is advantageous to avoid random initialization.

Layer init.	Prompt init.	HMDB	UCF	SSv2	All
CLIP	“a photo of a”	63.9	90.7	9.8	54.8
Random	“a photo of a”	63.5	90.5	9.9	54.6
CLIP	Random	62.5	90.2	9.5	54.1

average over all datasets, TC-CLIP shows distinct gaps from the baseline model ViFi-CLIP [26] by 3.5%p, 6%p, and 4.8%p in base, novel, and harmonic mean (HM), respectively.

B Temporal Subset Analysis

We adopt the temporal subset analysis suggested in [27] to further analyze the temporal modeling ability of trained models. In this setting, the temporal subset consists of specific action classes that require more temporal information to recognize them. After shuffling frames in time and measuring whether the human annotator can still recognize the action, the classes that cannot be recognized are added to the temporal subset. The resulting temporal classes in Kinetics-400 and SSv2 are a total of 32 classes and 16 classes, respectively. Table 10 compares the top-1 accuracy using full validation splits and the temporal subsets. We use fully-supervised models for Kinetics-400 and 16-shot-trained models for SSv2. Our model shows unique gains over ViFi-CLIP [26] for the temporally challenging videos, more than when evaluated across the entire validation set. This demonstrates the superiority of TC-CLIP in handling temporal information.

C More Ablation Study on VP

VP layer selection. Table 11 presents the ablation study on the layer selection in the VP module. We compare the few-shot classification accuracy by varying the layer indices of the text and vision inputs $\{L_{\text{text}}, L_{\text{vision}}\}$ in the VP module $f_{\theta_{\text{VP}}}(\mathbf{p}^{L_{\text{text}}-1}, \mathbf{s}_{\text{proj}}^{L_{\text{vision}}})$. We observe that applying conditional prompting at the early stage ($L_{\text{text}} = 1$) does not generalize well, regardless of the vision layer

index. This suggests the early-stage prompting design is hard to generalize in a full fine-tuning scenario, possibly because CLIP was initially trained in a vision-text late-alignment fashion. The middle- and late-stage prompting designs are also compared, and the last layer indices are finally chosen for both modalities.

VP initialization. Table 12 presents the ablation study on the initialization strategy of the VP layer and learnable prompt vectors. By default, we initialize the weight of the VP module using the weight from the last layer of the CLIP text encoder since randomly initializing it occasionally incurs unstable training results in the few-shot scenario. Similarly, it is beneficial to initialize the learnable prompt vectors using the prompt template “a photo of a” as generally done in the prompt tuning methods [17, 37].

D Impact of Weight-space Ensemble

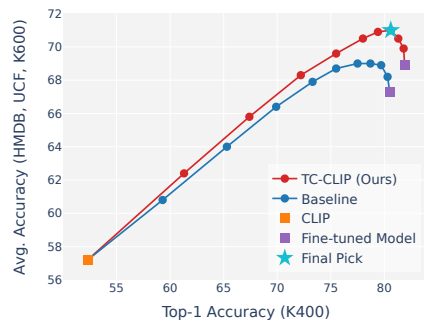


Fig. 8: Weight averaging ablation.

TC-CLIP achieves a better trade-off than the baseline as our curve is always on top of the baseline’s curve. This demonstrates that our model takes more advantages from weight ensembling. We choose $w = 0.7$ as our final ensemble ratio.

E More Visualizations of Context Tokens and Attentions

Context token visualization. Fig. 9 visualizes the seed tokens and context tokens from the last layer of the vision encoder in TC-CLIP. As can be seen, the seed tokens mainly consist of patch tokens from the most informative regions in each frame, which contain the foreground, such as a person, animals, hands, and objects. To visualize each context token, we colorize its corresponding source token positions using the average color of the input image patches of that region. It is noteworthy that a single context token (highlighted in red) successfully tracks and summarizes a specific object or part throughout the entire video.

Attention visualization. Fig. 10 visualizes the attention maps of TC-CLIP compared to ViFi-CLIP [26]. As shown in Fig. 10(a)–(b), TC-CLIP tends to focus more on dynamically moving parts, such as hands and arms, during the

In Fig. 8, we evaluate the effectiveness of weight ensembling by varying the ensemble ratio w from 0 to 1 with a step size of 0.1. Specifically, the backbone weights of both vision and text encoders are linearly interpolated between CLIP and fine-tuned model, *i.e.*, $\theta_w = (1-w) \cdot \theta_{\text{CLIP}} + w \cdot \theta_{\text{fine-tuned}}$. The y -axis displays the average accuracy on the zero-shot video datasets and the x -axis displays the accuracy on the fine-tuning dataset K-400. Our

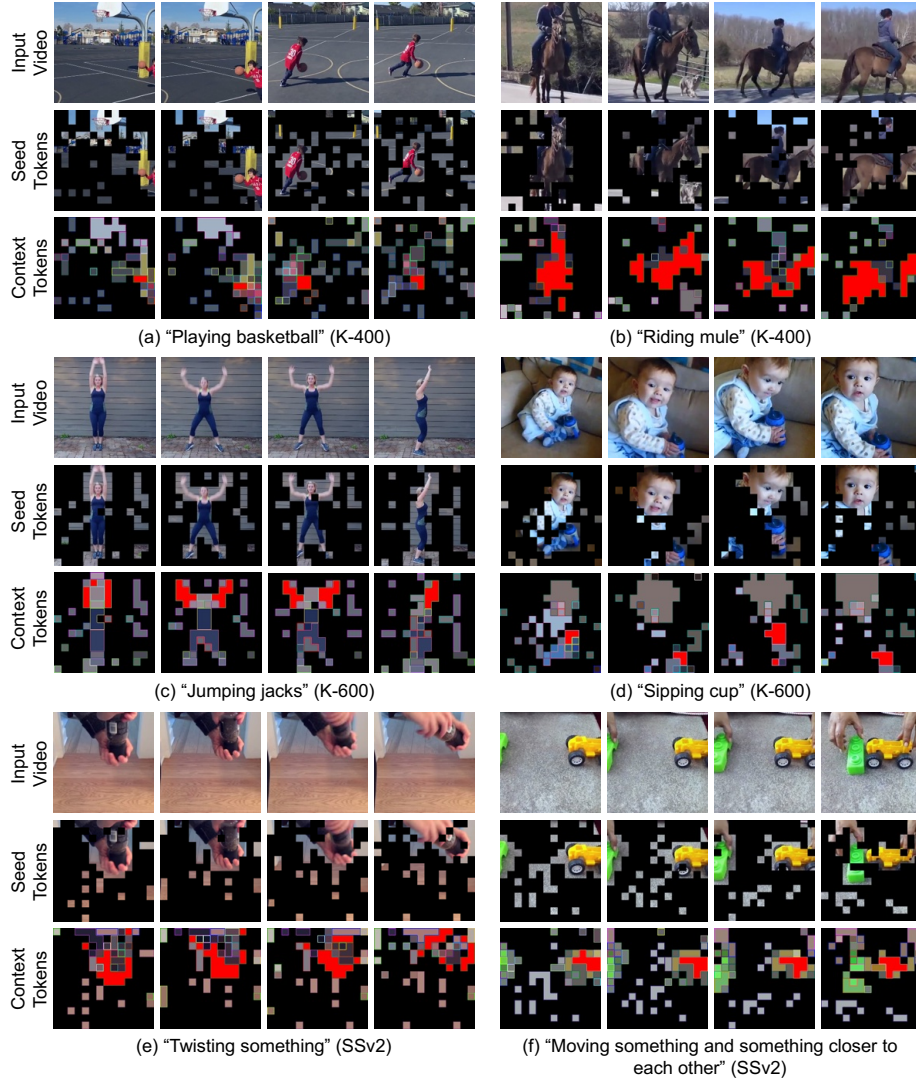


Fig. 9: Context token visualization of TC-CLIP on Kinetics-400, Kinetics-600, and SSv2 datasets. We visualize selected seed tokens and the resulting context tokens in the last layer of the vision encoder. Patch tokens with the same inner and border color are summarized into one context token. Regions highlighted in **red** represent a specific object or part grouped into a single context token throughout the video.

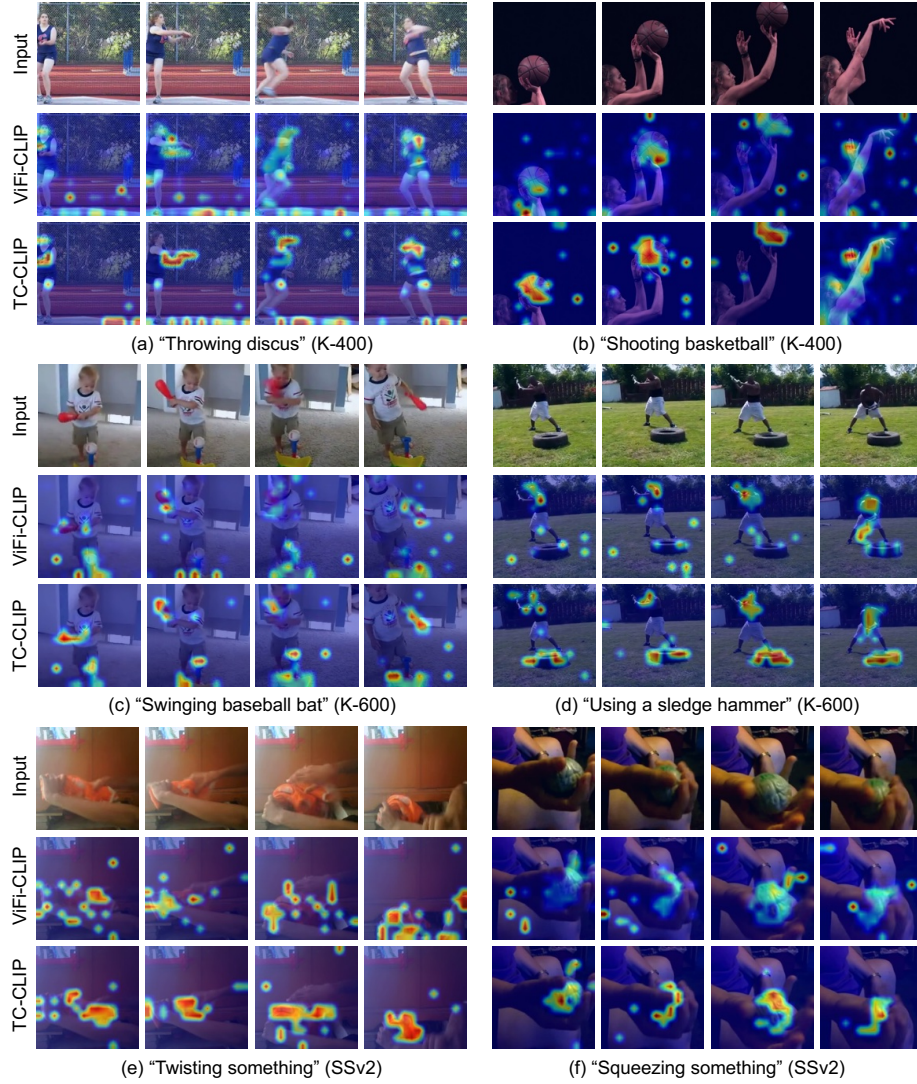


Fig. 10: Attention visualization of TC-CLIP in comparison with ViFi-CLIP [26] on Kinetics-400, Kinetics-600, and SSv2 datasets. (a)–(b): TC-CLIP tends to focus more on fast-moving parts such as hands and arms. (c)–(d): While ViFi-CLIP dominantly attends to the most salient regions, TC-CLIP attends to multiple objects based on inter-object relationships relevant to the occurring actions. (e)–(f): TC-CLIP consistently attends to the main object with deformations throughout the video.

action of throwing or shooting objects. Furthermore, TC-CLIP attends to multiple objects simultaneously based on inter-object relationships, as illustrated in Fig. 10(c)–(d). For example, during actions like “swinging baseball bat,” it effectively attends to both the bat and the baseball being struck. This highlights the TC-CLIP’s capability to understand complex interactions based on a temporal context in dynamic scenes, which is potentially more helpful than ViFi-CLIP, which only attends to the most salient region in each frame. Finally, Fig. 10(e)–(f) shows TC-CLIP’s consistent attention towards objects with deformations across video frames, which are more striking than ViFi-CLIP’s.

F Experimental Setup Details

F.1 Dataset Details

We conduct experiments over 5 action recognition benchmarks: Kinetics-400 [16] & 600 [2], HMDB-51 [18], UCF-101 [28], and Something-Something v2 (SSv2) [8].

Kinetics-400 [16] is a large-scale action recognition dataset with a total of 400 action classes, where its video clips are collected from YouTube and last for about 10 seconds. It contains around 240k training videos and 20k validation videos.

Kinetics-600 [2] is an extension of Kinetics-400 with approximately 480k video clips covering 600 action categories. The videos are divided into 390k for training, 30k for validation, and 60k for testing. We mainly adopt the validation split for zero-shot evaluation.

HMDB-51 [18] dataset includes 6,869 clips divided into 51 action categories. There are three individual splits for training and validation.

UCF-101 [28] is an action recognition dataset collected from YouTube, including 13,320 video clips with 101 action categories. Similar to HMDB-51, the training and test videos have three splits.

SSv2 [8] is a challenging dataset with 174 fine-grained action classes, which are more temporally biased than the other datasets. The standard split consists of 168,913 training videos and 24,777 validation videos.

F.2 Implementation Details

During the bipartite matching, we start with the seed tokens arranged based on the [CLS] token attention values in each frame. These tokens are then divided into two sets by alternating positions. Subsequently, r pairs of tokens with the highest cosine similarity are merged by averaging their features, and remaining two sets are then concatenated back together. This process is repeated iteratively, employing a constant r scheduling for every iteration with an exception in the final iteration to ensure that the number of final context tokens becomes k . Following [17, 37], the learnable prompts are initialized with the prompt “a photo of a”. For training recipes, we follow [26] for zero-shot, few-shot, and

fully-supervised settings and follow [9] for base-to-novel generalization. By default, we use the AdamW optimizer with momentum betas of (0.9, 0.98) and a weight decay of 0.001. The initial learning rate of the VP module is $10\times$ larger than the base learning rate in each setting. Training configurations and evaluation metrics in each protocol are specified below.

Zero-shot action recognition. The models are trained on Kinetics-400 and evaluated on HMDB-51, UCF-101, and Kinetics-600 datasets. For HMDB-51 and UCF-101, we report the average and standard deviation of top-1 accuracy across three official validation splits. In the case of Kinetics-600, we apply the zero-shot evaluation protocol from [3], which exploits 220 categories of Kinetics-600 that do not appear in Kinetics-400. We use the three splits provided by [3], each containing 160 categories. The results include the average top-1 and top-5 accuracy and their respective standard deviations. During the training, the base learning rate is set to 8×10^{-6} and is decayed to 8×10^{-8} following the cosine decay scheduler. The batch size is 256, and the total number of epochs is 10, including 5 linear warmup epochs.

Few-shot action recognition. We adopt the K -shot training splits from [26] that randomly samples $K = 2, 4, 8, 16$ videos from each class on HMDB-51, UCF-101, and SSv2. The models are evaluated using the first validation split of HMDB-51 and UCF-101 and the full validation split of SSv2. The base learning rate is set to 2×10^{-6} and is decayed to 2×10^{-8} . The batch size is 64, and the total number of epochs is set to 50, starting with 5 linear warmup epochs.

Base-to-novel generalization. We adopt the base and novel splits from [26]. The models are trained on a set of base (seen) classes in a few-shot manner and subsequently evaluated on a set of novel (unseen) classes for four datasets: Kinetics-400, HMDB-51, UCF-101, and SSv2. Each dataset comprises three training splits containing randomly sampled 16 shots of base action categories. We report the average accuracy over three splits. For HMDB-51 and UCF-101, the training and validation consider only their first split, whereas, for Kinetics and SSv2, the models are evaluated on their full validation split. The base learning rate is set to 3.33×10^{-6} and is decayed to 3.33×10^{-8} . The batch size is 64. The number of epochs is 12, including 2 warmup epochs.

Fully-supervised action recognition. The models are trained on Kinetics-400 and evaluated on its complete validation split. The base learning rate is set to 2.2×10^{-5} and is decayed to 2.2×10^{-7} following the cosine decay scheduler. The batch size is 512, and the total epochs is 30 epochs, including 5 linear warmup epochs.